RhoA and MAPK signal transduction pathways regulate NHE1-dependent proximal tubule cell apoptosis after mechanical stretch

Victoria Bocanegra,[1] Andrea Fernanda Gil Lorenzo,[1] Valeria Cacciamani,[2] María Eugenia Benardón,[2] Valeria Victoria Costantino,[1] and Patricia G. Vallés[1,2]

[1]*Instituto de Medicina y Biología Experimental de Cuyo-Consejo Nacional de Investigaciones Científicas y Técnicas, Buenos Aires, Argentina; and* [2]*Área de Fisiología Patológica, Departamento de Patología, Facultad de Ciencias Médicas, Universidad Nacional de Cuyo, Mendoza, Argentina*

Bocanegra V, Gil Lorenzo AF, Cacciamani V, Benardón ME, Costantino VV, Vallés PG. RhoA and MAPK signal transduction pathways regulate NHE1-dependent proximal tubule cell apoptosis after mechanical stretch. *Am J Physiol Renal Physiol* 307: F881–F889, 2014. First published July 30, 2014; doi:10.1152/ajprenal.00232.2014.—Mechanical deformation after congenital ureteral obstruction is traduced into biochemical signals leading to tubular atrophy due to epithelial cell apoptosis. We investigated whether Na^+/H^+ exchanger 1 (NHE1) could be responsible for HK-2 cell apoptosis induction in response to mechanical stretch through its ability to function as a control point of RhoA and MAPK signaling pathways. When mechanical stretch was applied to HK-2 cells, cell apoptosis was associated with diminished NHE1 expression and RhoA activation. The RhoA signaling pathway was confirmed to be upstream from the MAPK cascade when HK-2 cells were transfected with the active RhoA-V14 mutant, showing higher ERK1/2 expression and decreased p38 activation associated with NHE1 downregulation. NHE1 participation in apoptosis induction was confirmed by specific small interfering RNA NHE1 showing caspase-3 activation and decreased Bcl-2 expression. The decreased NHE1 expression was correlated with abnormal NHE1 activity addressed by intracellular pH measurements. These results demonstrate that mitochondrial proximal tubule cell apoptosis in response to mechanical stretch is orchestrated by signaling pathways initiated by the small GTPase RhoA and followed by the opposing effects of ERK1/2 and p38 MAPK phosphorylation, regulating NHE1 decreased expression and activity.

Na^+/H^+ exchanger 1; RhoA; mitogen-activated protein kinases; apoptosis; proximal tubule cell; mechanical stretch

MECHANICAL STRETCHING of the tubular epithelium, caused by retrograde pressure shifts, is regarded as a highly significant step in the progression of obstructive nephropathy. Tubular stretching resulting in an axial strain might be produced by unilateral ureteral obstruction (UUO) through a mechanical signal (6) that triggers the destruction of renal tubular cells by apoptosis leading to tubular atrophy, a hallmark of renal disease progression (15). Previously, we have shown that apoptosis induction is the mechanism involved in tubular atrophy after 14 days of rat neonatal UUO, including Bcl-2 downregulation and caspase 3 activation (3). A number of important pathophysiological conditions are associated with tissue damage due to shrinkage-induced cell death, yet the mechanisms leading from mechanical deformation to cell death are still incompletely understood. Ubiquitous Na^+/H^+ ex-changer 1 (NHE1) is expressed on the basolateral plasma membrane of epithelial cells (16) and is normally quiescent (18, 20). NHE1 activation counteracts apoptosis through Na^+ influx and H^+ extrusion, resulting in the restoration of cell volume and cytosolic pH, respectively. However, with overwhelming or sustained apoptotic stimuli, the prosurvival NHE1 effect can be surmounted, which allows cells to proceed toward apoptosis. A property of NHE1 is that it associates with multiple binding partners, forming a macromolecular complex that appears to function as a scaffold for a variety of signaling events. A cell's ability to strengthen itself in response to an applied force depends on focal adhesion assembly where the force is applied (21). Force-induced assembly of focal adhesions is mediated by activation of Rho and its downstream targets (28). Rho regulates the assembly of focal adhesions in adherent cells through activation of Rho kinase/Rho-associated coiled-coil forming protein kinase (ROCK) and other effectors. A study (10) in fibroblasts has shown that NHE1 plays a direct role in controlling actin dynamics and subsequent motility through a protein-protein interaction with the cytoskeletal adaptor protein ezrin and that, in those cells, RhoA-dependent modulation of cytoskeletal dynamics and motility occurred via direct regulation of NHE1 activity. Regulation of NHE1 activity by MAPKs appears to involve direct phosphorylation, where the Ser^{703} residue is directly phosphorylated by ERK effector p90 ribosomal S6 kinase (2), and NHE1 has also been proposed to be directly phosphorylated by p38 MAPK (19). Interestingly, recent reports have suggested that NHE1 plays a central role in the regulation of MAPK activity after certain stimuli, yet the effects of NHE1 on MAPK activity are highly context and cell type specific. The present study was undertaken to further investigate the signal transduction system(s) involved in NHE1-associated apoptosis induction after mechanical stretch in a renal human epithelial cell line (HK-2 cells). In light of these findings, we postulate that persistent mechanical stress triggers cell apoptosis as a result of diminished NHE1 expression and activity; this exchanger is regulated by upstream RhoA activity and opposing effects of ERK1/2 and p38 MAPK signaling transduction pathways.

MATERIALS AND METHODS

Cell culture and chemicals. HK-2 cells (29), an immortalized human proximal tubule cell line, were obtained from American Type Culture Collection and grown in DMEM-F-12 culture medium (GIBCO, Invitrogen) containing 10% FBS (GIBCO, Invitrogen) and 1% penicillin-streptomycin in a regular CO_2 incubator at 37°C. HK-2 cells were used in all experiments described here.

Address for reprint requests and other correspondence: P. G. Vallés, Área de Fisiología Patológica, Departamento de Patología, Facultad de Ciencias Médicas, Universidad Nacional de Cuyo, Centro Universitario, Mendoza CP: 5500, Argentina (e-mail: pvalles@fcm.uncu.edu.ar).

Cyclic stretch. HK-2 cells were cultured in a mechanically active environment that involves the application of a controlled vacuum to the under surface of culture plates with deformable bases to generate cellular stretch (30). HK-2 cells were seeded on collagen type I (Sigma-Aldrich)-coated 25-mm six-well flexible or rigid based plates. The device was placed at 37°C and 5% CO_2 in a humidified incubator. Vacuum (22.3 kPa) was cyclically applied to subconfluent cells, inducing a 25% uniaxial elongation on the flexible surface where the culture cells are attached; this induced cyclic stretch, alternating cycles of 5 s of stretch and 5 s of relaxation at a rate of 6 cycles/min (frequency: 30 cycles/min, with a stretch-to-relaxation relation of 1:1). Stretch and control experiments were carried out simultaneously with cells derived from a single pool. Stretched cells were harvested at different time points that included 15, 90, and 180 min of mechanical stretch.

Annexin V/propidium iodide staining assay. Apoptosis was examined by detecting phosphatidylserine exposure on cell membrane with annexin V (4). Stretched and control HK-2 cells were simultaneously stained with annexin V-FITC and propidium iodide (PI) according to the manufacturer's recommendation (BD Biosciences). Flow cytometry analysis was performed using a FACSAria III cytometer (Becton Dickinson). A total of at least 20,000 events were analyzed per sample. Data were analyzed using FACSDiva software (Becton Dickinson).

Cell fractioning and immunoblot analysis. Stretched and control HK-2 cell suspensions were subjected to three cycles of freezing and thawing. Nuclei and nonlysed cells were pelleted at 1,000 *g* for 10 min at 4°C. The supernatant was centrifuged at 100,000 g for 60 min at 4°C. The membrane fraction contained in the pellet was resuspended in lysis buffer (14). The supernatant was designated as the cytosolic fraction. Protein content was determined by the Bradford technique (5). Equal amounts of protein were treated with Laemmli's buffer, separated by SDS-PAGE, transferred to nitrocellulose membranes, and treated as previously described (3). Membranes were incubated overnight with mouse monoclonal Bcl-2 (Sigma-Aldrich), caspase 3 (Promega), NHE1 (Chemicon), RhoA (Santa Cruz Biotechnology), phosphorylated (p-)ERK (Santa Cruz Biotechnologu), ERK2 (Santa Cruz Biotechnology), p-p38 (Sigma-Aldrich), p38 (Sigma-Aldrich), α-tubulin (Sigma-Aldrich), and GAPDH (Sigma-Aldrich). Densitometric analysis of bands was performed using ImageJ software. The magnitude of the immunosignal was given as a percentage of control HK-2 cells.

Cell transfection. HK-2 cells were transfected with small interfering (si)RNA duplex against NHE1 (0.75 µg/100 µl, Santa Cruz Biotechnology) using Lipofectamine 2000 (Invitrogen) according to the manufacturer's protocol. For the RhoA assay, cells were cotransfected with pEGFP-RHOA wild type (WT), pEGFP-RHOA-V14, or pEGFP-RHOA-N19. After transfection, cells were allowed to synthesize proteins under regular conditions for 24, 48, and 72 h. The efficiency of NHE1 silencing was measured using immunofluorescence microscopy and Western blot assay.

Immunofluorescence staining. Control and NHE1 siRNA-transfected HK-2 cells were fixed with 3% paraformaldehyde in PBS for 10 min at 37°C, washed, and blocked with 50 mM NH_4Cl in PBS. Cells were then permeabilized with 0.05% saponin (Sigma-Aldrich) in PBS containing 0.5% BSA (Sigma-Aldrich) and incubated with primary antibody against NHE1. After being washed, cells were incubated with secondary antibody conjugated with FITC (Jackson ImmunoResearch Laboratories). HK-2 cells were mounted with Mowiol (Sigma-Aldrich) and examined by confocal microscopy using an FV1000 Olympus confocal microscope and FV 10-ASW 1.7 software (Olympus). Images were processed using ImageJ software.

Inhibition assay. To study the participation of the MAPK signaling pathways involved in stretch-induced apoptosis, specific pharmacological inhibitors [p38 MAPK inhibitor SB-203598 (30 µM, Invitrogen), ERK1/2 inhibitor PD-98059 (30 µM, Invitrogen), and ROCK inhibitor Y-27632 (10 µM, Sigma-Aldrich)] were resuspended to an adequate concentration in DMSO and added to HK-2 cells for 1 h. For NHE1 inhibition activity, we used 5′-(*N*-ethyl-*N*-isopropyl)amiloride [EIPA (30 µM, Sigma-Aldrich)]. DMSO alone was used as a mock control.

Intracellular pH measurements. For intracellular pH (pH_i) measurements, HK-2 cells were seeded on coverslips and transferred to a perfusion chamber. The temperature of the chamber was maintained at 37 ± 0.5°C. The control bath solution was initially a standard HEPES solution. HK-2 cells were loaded with the pH-sensitive dye BCECF (10 µM) for 20 min as previously described (13). pH_i was measured microfluorometrically by exciting the dye alternately at 490 and 440 nm while monitoring the emission at 532 nm with a video-imaging system. To measure NHE1 activity (Na^+-dependent pH_i recovery), Na^+-HEPES was used. To measure Na^+-independent pH_i recovery, bicarbonate-free solution was used and Na^+ was removed to abolish NHE activity; for these experiments, Na^+ was replaced by *N*-methyl-D-glucamine. To induce strong intracellular acidification and activate NHE1, the NH_4Cl prepulse technique was used in the presence of Na^+, as previously described (31). All chemicals were obtained from Sigma-Aldrich. Each experiment was calibrated for pH_i using the nigericin/high-K^+ method, and the obtained ratios were converted to pH_i. Na^+-dependent pH_i recovery rates in response to an acid load were calculated in HK-2 cells in the pH range of 6.80–7.00. Data are provided as means $\pm$ SE; *n* represents the number of cells investigated.

Statistical analysis. Results were assessed by one-way ANOVA for comparisons among groups. Differences among groups were determined by a Bonferroni posttest. Results are given as means $\pm$ SE from three independent experiments. Statistical tests were performed using GraphPad (version 5.00) for Windows XP (GraphPad software). *P* values of <0.05 were considered significant.

RESULTS

Mechanical stretch induced apoptosis in HK-2 cells in a time-dependent manner. We characterized stretch-induced apoptosis in HK-2 cells using annexin V/PI dual staining by flow cytometry. When mechanical stretch was applied to HK-2 cells (Fig. 1*A*), we observed apoptosis induction in a time-dependent manner with an increase in the percentage of annexin V^+ HK-2 cells (33.1% at 90 min and 45.8% at 180 min) compared with control cells (0.3% annexin V^+ cells). To determine if apoptosis induction in response to mechanical stretch involves the caspase cascade, control and stretched HK-2 cell lysates were probed for Bcl-2 and caspase 3 protein expression using Western blot analysis. We observed a downregulation in Bcl-2 expression (Fig. 1B) and a progressive increase in caspase 3 protein levels after 90 and 180 min (Fig. 1*C*), demonstrating a time-dependent increase apoptosis induction in response to stretch.

Cyclic stretch induces diminished NHE1 expression in HK-2 cells followed by apoptosis induction. To determine the relationship between mechanical injury and the NHE1 response, HK-2 cells were subjected to increasing cyclic stretch, and cell lysates were used in immunoblot analysis. We observed a progressive decrease in NHE1 protein expression after applying mechanical deformation, of which the maximum decrease was at 180 min of cell stretch (Fig. 2*A*). The apoptotic response to mechanical stretch associated with a progressive decrease of NHE1 suggests a role of NHE1 in cell survival. To further determine if NHE1 has a direct participation on apoptosis induction independently of mechanical deformation, siRNA-mediated knockdown of NHE1 was performed in control HK-2 cells. NHE1 expression was assessed after 24, 48, and 72 h
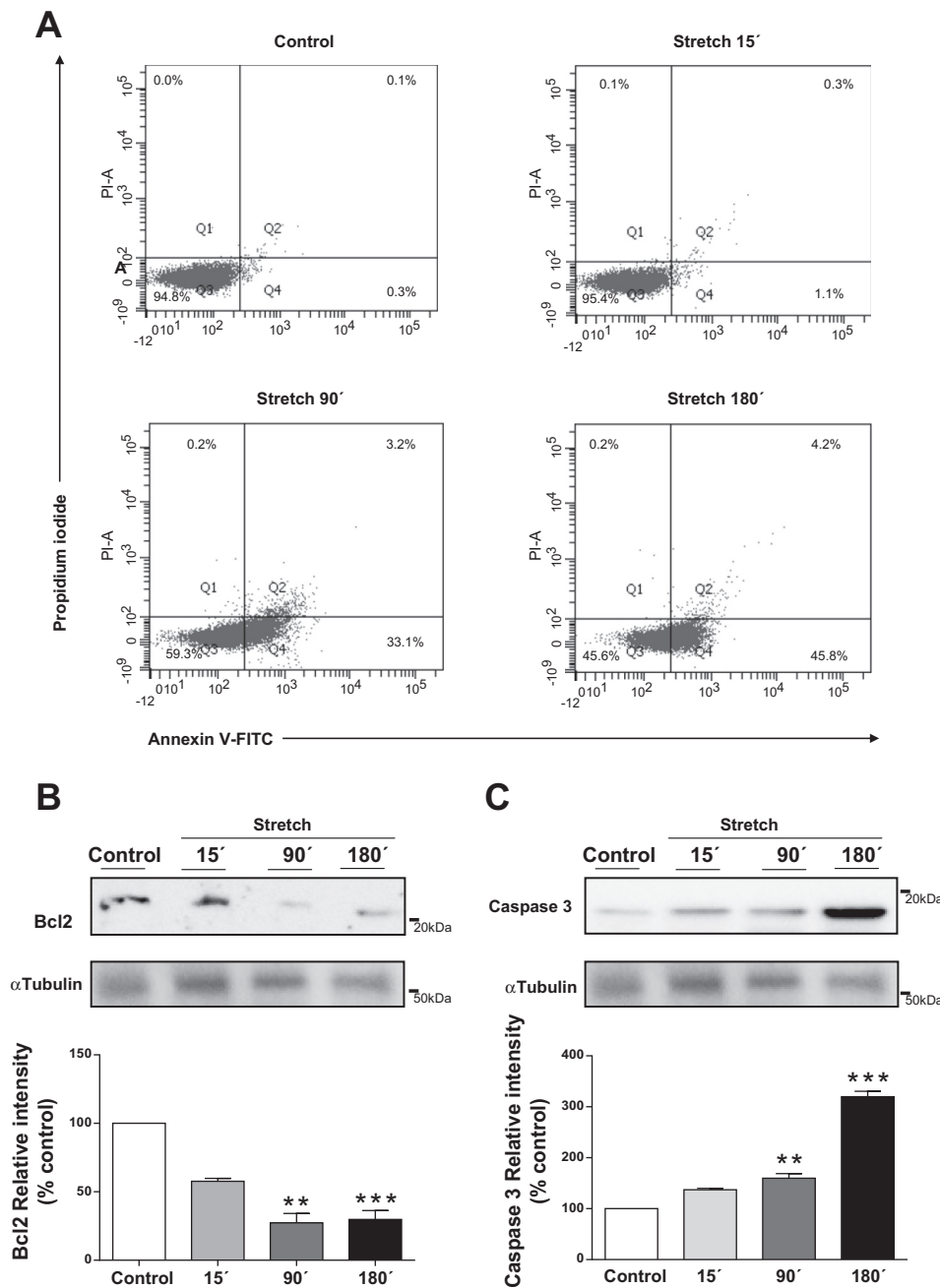
Fig. 1. Effect of cyclic stretch-induced apoptosis on HK-2 cells. HK-2 cells subjected to 15, 90, and 180 min of cyclic stretch were collected to be analyzed for apoptosis induction using flow cytometry and Western blot techniques. *A*: control and stretched cells were costained with propidium iodide (PI) and annexin V-FITC and analyzed using a FACS AriaIII cytometer. In each plot, the *bottom left* quadrant (Q3) represents viable cells (annexin V^-FITC$^-$/PI$^-$), the *top left* quadrant (Q1) represents necrotic cells (annexin V-FITC$^-$/PI$^+$), the *bottom right* quadrant (Q4) represents early apoptotic cells (annexin V-FITC$^+$/PI$^-$), and the *top right* quadrant (Q2) represents late apoptotic cells (annexin V-FITC$^+$/PI$^+$). The numbers in each plot show the percentages of cells in the quadrant. A representative profile of three independent experiments is shown. *B* and *C*: Western blot analysis of Bcl-2 (*B*) and caspase 3 (*C*) in control and stretched HK-2 cell lysates. A representative blot from three independent experiments is shown. Tubulin was used as a control for protein loading. Expression levels were determined using densitometric analysis. Data are expressed as means $\pm$ SE; $n = 3$. $**P < 0.01$. $***P < 0.001$.

posttransfection using Western blot analysis. Seventy-two hour posttransfection, we observed significant decreased of NHE1 protein expression (Fig. 2*B*). The diminished NHE1 expression was also corroborated by immunofluorescence (Fig. 2*C*). After 72 h of NHE1 siRNA, we observed a subsequent decreased of Bcl-2 protein expression and higher caspase 3 protein levels compared with nontargeting siRNA (control), demonstrating a direct involvement of NHE1 in mitochondrial pathway activation and apoptosis induction (Fig. 2, *D* and *E*, respectively).

NHE1 manipulation induces higher apoptosis cell induction after mechanical stretch. To demonstrate the NHE1 contribution to cell apoptosis induction in response to mechanical stretch, HK-2 cells were incubated either with EIPA (30 μM) for 60 min (Fig. 3*A*) or transfected with NHE1 siRNA for

72 h (Fig. 3*B*) and subjected to 90 and 180 min of mechanical stretch and collected to be analyzed by flow cytometry. After selective blockade of NHE1 activity with EIPA, we observed 20.4% of apoptotic cells (annexin V^+) and 10.8% of later apoptosis (annexin V^+/PI$^+$) after 90 min of cyclic stretch and 27.8% of apoptosis (annexin V^+) and 34.9% of later apoptosis (annexin V^+/PI$^+$) after 180 min of cell stretch (Fig. 3*A*). After siRNA knockdown of NHE1 protein expression on HK-2 cells and subsequent cyclic stretch, flow cytometry annexin V/PI staining measurements showed 21.3% of early apoptosis (annexin V^+/PI$^-$) and 19.6% of later apoptosis (annexin V^+/PI$^+$) after 90 min of cyclic stretch (Fig. 3*B*). After 180 min of mechanical deformation, apoptosis induction increases by 16.3% of early apoptosis (annexin V^+/PI$^-$) and 58% in later

Fig. 2. Apoptosis induction in response to Na$^+$/H$^+$ exchanger 1 (NHE1) downregulation. *A*: Western blot analysis of NHE1 protein abundance of HK-2 cells subjected to 15, 90, and 180 min of cyclic stretch. A representative blot from three independent experiments is shown. Tubulin was used as a control for protein loading. *B*: HK-2 cells were transfected with 0.75 μg small interfering (si)RNA/100 μl Lipofectamine targeted to either a nonrepresented sequence (control) or NHE1 and then incubated for 24, 48, and 72 h. The amount of NHE1 protein was determined by immunoblot analysis. Using densitometric analysis, 72 h of siRNA showed significantly reduced protein levels compared with 40% of control. *C*: transfected HK-2 cells with NHE1 siRNA were analyzed using indirect immunofluorescence. Images were quantified and showed a 60% decrease in transfected HK-2 cells versus control (**$P < 0.01$, NHE1 siRNA vs. control). Images were taken using a confocal microscope (FV-1000, Olympus). Bar = 20 μm. *D*: cell lysates from transfected HK-2 cells were probed for Bcl-2 and caspase 3 using Western blot techniques. Protein levels on Western blots were determined using densitometric analysis. Data are expressed in the corresponding bar graph as means ± SE; $n = 3$. *$P < 0.05$. **$P < 0.01$. ***$P < 0.001$.
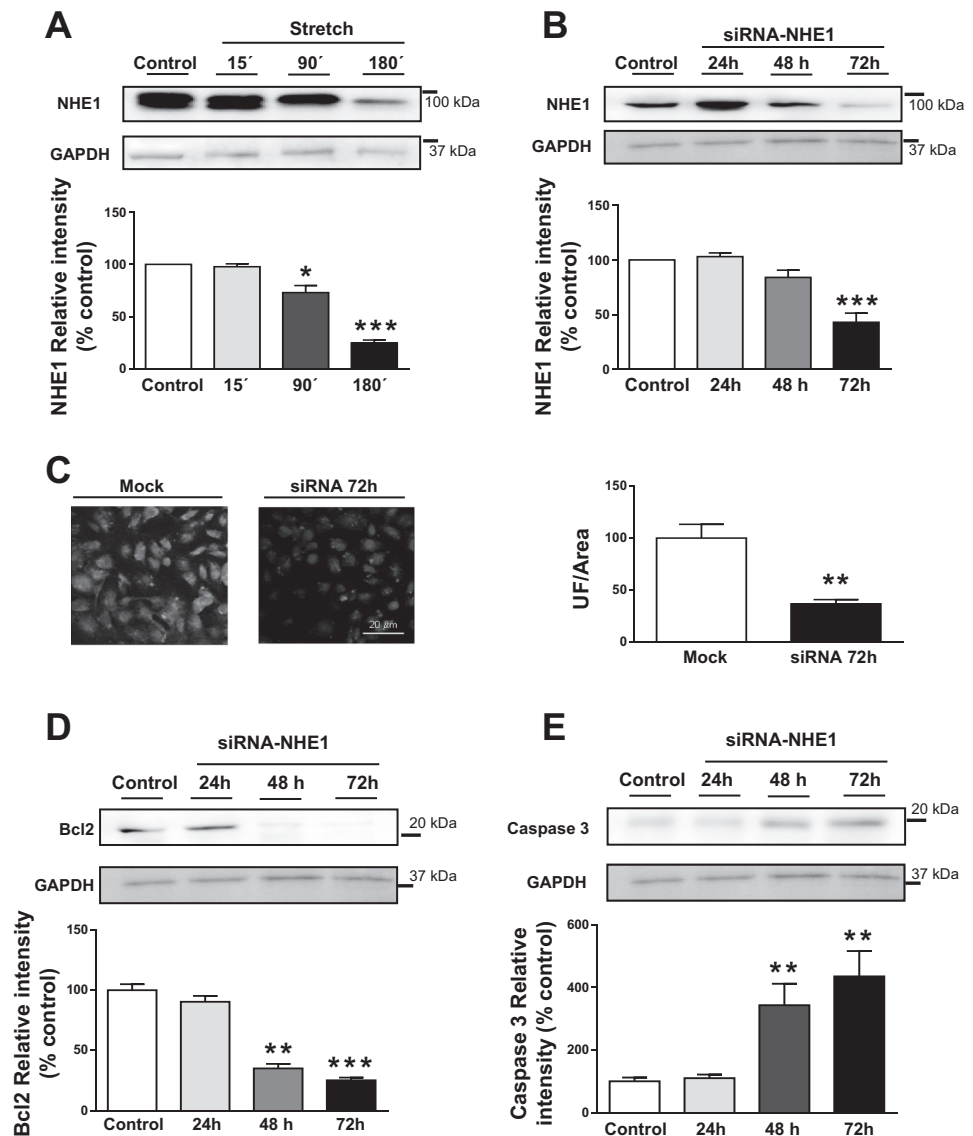
apoptosis (annexin V$^+$/PI$^+$). These results reveal that both activity and expression contribute to counteract the cellular insult generated by mechanical deformation.

Progressive time-dependent RhoA activation after cyclic stretch regulates NHE1. To analyze the expression of activated membrane-bound RhoA, HK-2 cells were exposed to increasing time periods of cyclic stretch. RhoA was highly activated after 15 min of cyclic stretch, with maximal protein levels of membrane-bound RhoA after 90 min of cell stretch (Fig. 4*A*). To verified if the RhoAGTPase signaling pathway was involved in NHE1 downregulation, pharmacological inhibitors as well as dominant negative and constitutively active mutants were probed. Cell lysates of HK-2 cells coexpressing EGFP-RHOA WT or the mutants EGFP-RHOA-V14 (a constitutive active mutant) or EGFP-RHOA-N19 (a constitutive inactive mutant) were probed using the Western blot technique to analyze the expression of NHE1. Inactivation of RhoA with the dominant negative N19RhoA mutant induced higher expression of NHE1 protein, whereas activating RhoA with constitutively active EGFP-RHOA-V14 reduced NHE1 protein

abundance compared with control HK-2 cells (Fig. 4*B*). Since ROCK has been proposed as a RhoA downstream effector, we studied the ROCK inhibitor response in HK-2 cells. Similar to the results observed after transfection with the dominant negative EGFP-RHOA-N19 mutant, ROCK inhibition induces higher abundance of NHE-1 protein abundance (Fig. 4*B*). These data show RhoA activation as an integral part of the signal transduction pathway involved in NHE1 downregulation.

Time-dependent cyclic stretch on ERK1/2 and p38 MAPK expression contributing to NHE1 regulation and apoptosis induction. Since MAPK activation has previously been involved in NHE1 regulation in other cell types, we examined the time course of ERK1/2 and p38 activation in cyclic stretched HK-2 cells. After 15 min of stretch, we observed an early increase in p-ERK1/2 protein levels followed by significantly decreased expression of ERK1/2 protein levels after 180 min of cyclic stretch (Fig. 5*A*). In contrast, a progressive increase in p-p38 protein abundance, with a maximum phosphorylation state after stretch for 180 min, was shown in HK-2
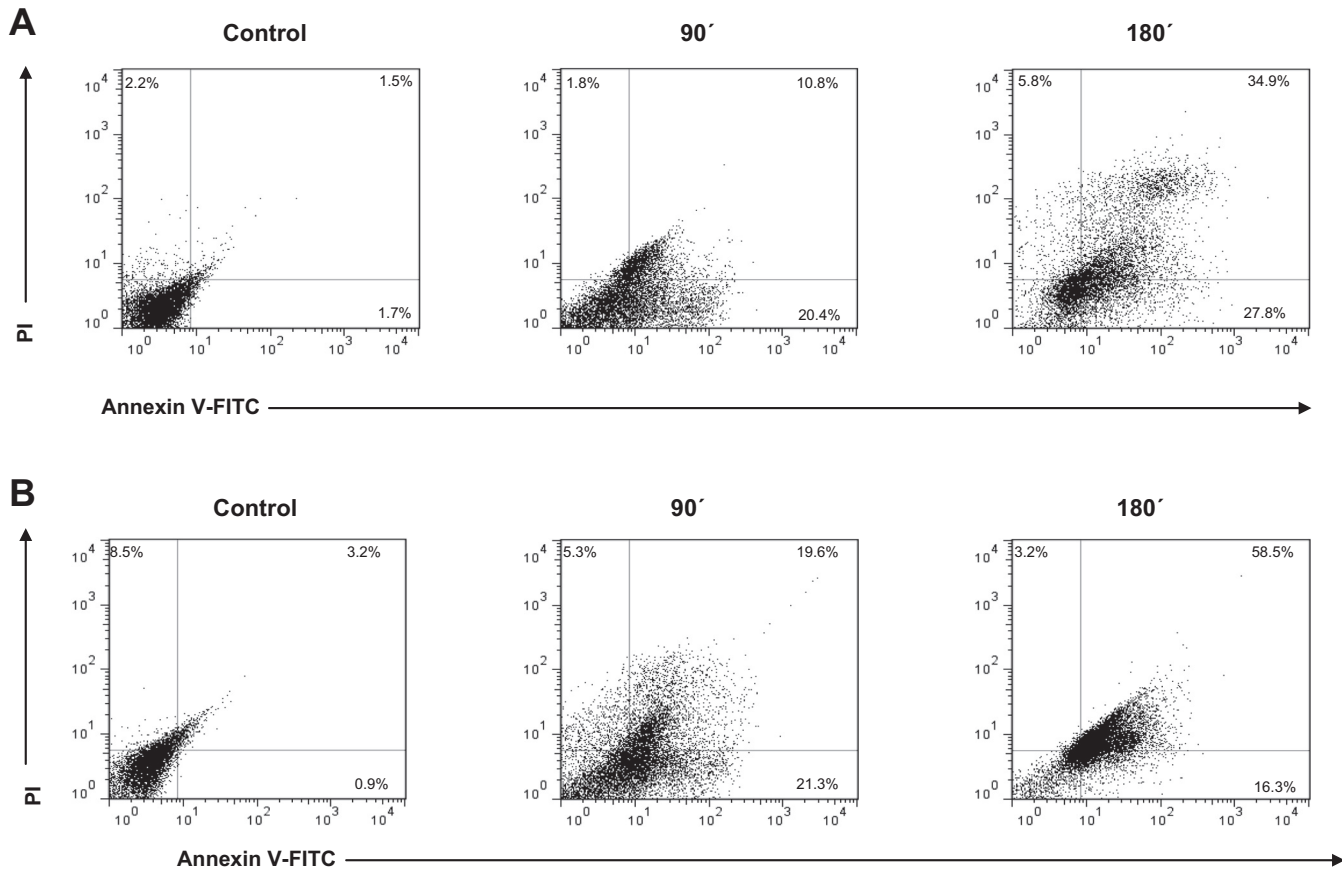
Fig. 3. NHE1 targeting induces higher apoptosis after cyclic stretch. HK-2 cells were seeded in collagen type I-coated plates, incubated with NHE1 inhibitor 5'-(N-ethyl-N-isopropyl)amiloride (EIPA; 30 µM) for 60 min or DMSO alone as mock control (control; A) or transfected with 0.75 µg siRNA/100 µl Lipofectamine targeted to either a nonrepresented sequence (control) or NHE1 for 72 h (B). Cells were subsequently subjected to 90 and 180 min of mechanical stretch. Control and stretched cells were collected and colabeled with annexin V-FITC/PI to quantify cell apoptosis by low cytometry using a FACSAriaIII cytometer. In each plot, the *bottom left* quadrant represents viable cells (annexin V$^-$FITC$^-$/PI$^-$), the *top left* quadrant represents necrotic cells (annexin V-FITC$^-$/PI$^+$), the *bottom right* quadrant represents early apoptotic cells (annexin V-FITC$^+$/PI$^-$), and the *top right* quadrant represents late apoptotic cells (annexin V-FITC$^+$/PI$^+$). The numbers in each plot show the percentages of cells in the quadrant.

cells compared with control cells (Fig. 5B). To establish if ERK1/2 and p38 MAPK signaling pathways have a direct involvement on NHE1 expression and apoptosis induction independently from stretch-induced regulation, we examined the effect of a panel of specific MAPK inhibitors. HK-2 cells were incubated with NHE1 inhibitor, ERK1/2 inhibitor, and p38 inhibitor for 60 min. Cell lysates were probed

using Western blot analysis to address NHE1 and caspase 3 protein levels. Treatment with the specific p38 inhibitor increased NHE1 expression (Fig. 5C) with an absence of caspase 3 expression, whereas persistent lower NHE1 protein levels and increased caspase 3 expression (Fig. 5D) were shown after ERK1/2 inhibition. These results indicate that apoptosis induction in HK-2 cells is mediated through
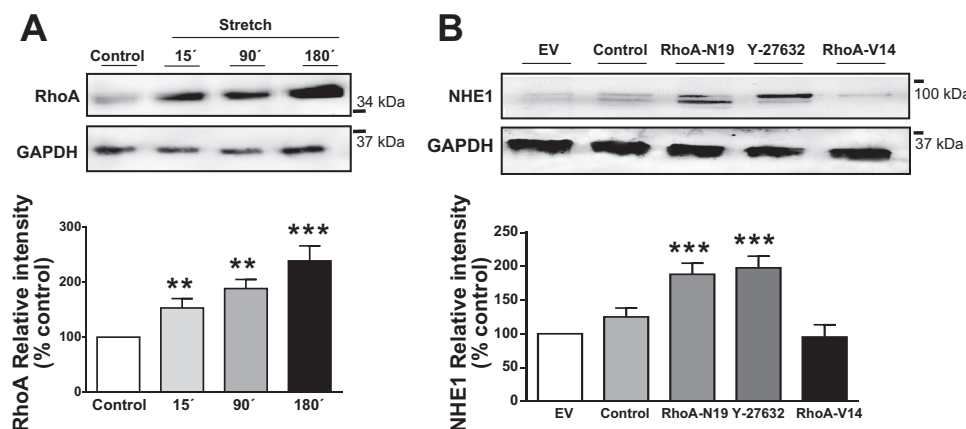

Fig. 4. RhoA signal transduction pathway. *A*: HK-2 cells were subjected to 15, 90, and 180 min of mechanical stretch, and Western blot analysis of the membrane fraction from cell lysates was performed to analyze membrane-bound RhoA. *B*: NHE1 expression was analyzed in HK-2 cells transfected with RhoA dominant negative vector (pEGFP-RHOA-N19) or RhoA active mutant (pEGFP-RHOA-V14) or incubated with Rho kinase (ROCK) inhibitor Y-27632 (10 µM). Protein levels on Western blots were determined using densitometric analysis. Data are expressed in the corresponding bar graph as means ± SE; $n = 3$. **$P < 0.01$. ***$P < 0.001$.

Fig. 5. Cyclic stretch effect on MAPK activity and its contribution to NHE1 regulation and apoptosis induction. HK-2 cells were submitted to 15, 90, and 180 min of cyclic stretch. Cell extracts were analyzed by Western blot analysis for both the phosphorylation state and total expression levels of ERK1/2 and p38 MAPK using phosphorylated (p-)ERK- and p-p38-specific antibodies. A and B: representative Western blots corresponding to stretch-induced ERK1/2 (A) and p38 (B) phosphorylation states. Membranes were stripped and reprobed with total ERK1/2 antibody and total p38 antibody. C: serum-starved HK-2 cells were incubated NHE1 inhibitor (EIPA; 50 μM), MEK1 inhibitor [PD-98059 (PD); 30 μM], and p38 inhibitor [SB-203589 (SB); 30 μM] for 60 min. NHE1 and caspase 3 expression were analyzed using Western blot analysis. Tubulin was used as a loading control. Expression levels on Western blots were determined using densitometric analysis. Data are expressed in the corresponding bar graph as means ± SE; $n = 3$. $*P < 0.05$. $**P < 0.01$. $***P < 0.001$.
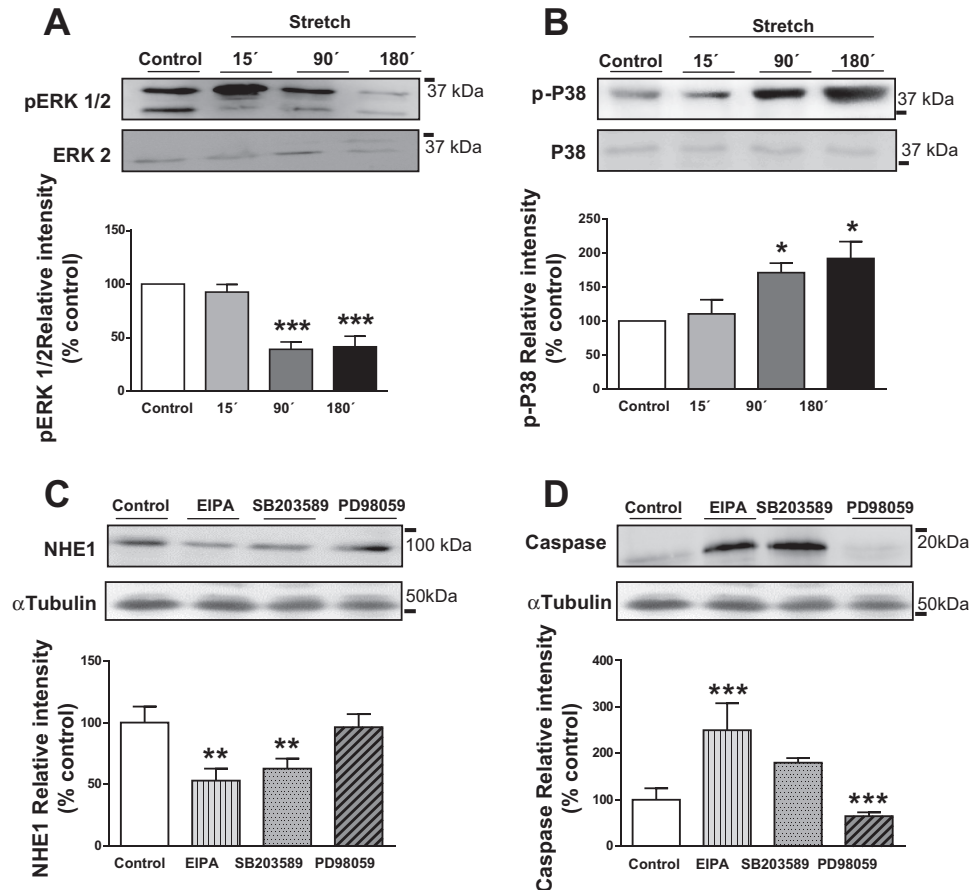
NHE1 downregulation in response to p38 MAPK signaling pathway activation.

Cross-talk between RhoAGTPase and MAPK pathways. Since we have shown that the ERK1/2 phosphorylation state diminished and p38 MAPK activity increased after cyclic stretch, we studied whether activation of RhoA after mechanical stretch could be involved in MAPK regulation. HK-2 cells coexpressing EGFP-RHOA WT or the mutants EGFP-RHOA-N19 or EGFP-RHOA-N19 were incubated for 3 h at 37°C. After RhoA inhibition, there were no significant changes in ERK1/2 or p38 expression; however, when the constitutively activ RhoA protein mutant was expressed in HK-2 cells, ERK1/2 activation was suppressed (Fig. 6A) and p38 MAPK activity was increased (Fig. 6B). To verify that RhoA was upstream of the MAPK pathway, HK-2 cells were incubated with MEK1 inhibitor, p38 inhibitor, and NHE1 inhibitor. Membrane fractions from the cell lysate were probed using the Western blot technique to analyze the expression of activated membrane-bound RhoA (Fig. 6C). After NHE1 inhibition, ERK1/2 inhibition, and p38 inhibition, there were no significant changes in activated RhoA protein expression, demonstrating that RhoA activation precedes the MAPK pathway activation that finally modifies NHE1 expression.

NHE1 activity in response to different signaling pathway inhibitors. We analyzed if NHE1 protein downregulation in response to RhoA and MAPK pathways was in accordance with NHE1 activity. Consequences of pharmacological inhibition of MEK1/2, p38, and ROCK were investigated. In control HK-2 cells, there was a rapid pH$_i$ recovery after acid loading (Fig. 7). To confirm the absence of NHE1 activity in EIPA-treated HK-2 cells, we determined pH$_i$ recovery, which showed no measurable Na$^+$-dependent pH$_i$ recovery from an acid load (Fig. 7). To analyze whether ERK1/2 was involved in pH$_i$ regulation, cells were exposed to ERK1/2 inhibitor for 30 min. We found lower Na$^+$-dependent pH$_i$ recovery rates compared with control cells. In contrast, preincubated HK-2 cells with p38 inhibitor demonstrated no difference in the Na$^+$-dependent pH$_i$ recovery rate compared with control cells. A similar pattern was observed when HK-2 cells were incubated with ROCK inhibitor, which showed a Na$^+$-dependent pH$_i$ recovery rate similar to control cells.

DISCUSSION

The data presented demonstrate apoptosis induction in HK-2 cells by mitochondrial pathway activation in response to cyclic stretch over increased periods of time. We provide direct evidence demonstrating that RhoA, p38, and ERK1/2 are involved in the NHE1 downregulation that leads to apoptosis induction after mechanical stretch. These results allow us to claim that stretch-induced cellular apoptosis in HK-2 cells could have physiological relevance in tubular atrophy observed in UUO. Physiological and pathological damage have been well studied in vivo models of UUO, demonstrating that tubular distention and apoptosis of renal tubular epithelial cell result in tubular atrophy, a hallmark of renal disease progression (15). During the first period of UUO, proximal tubule hydrostatic pressure increases are transmitted back to the
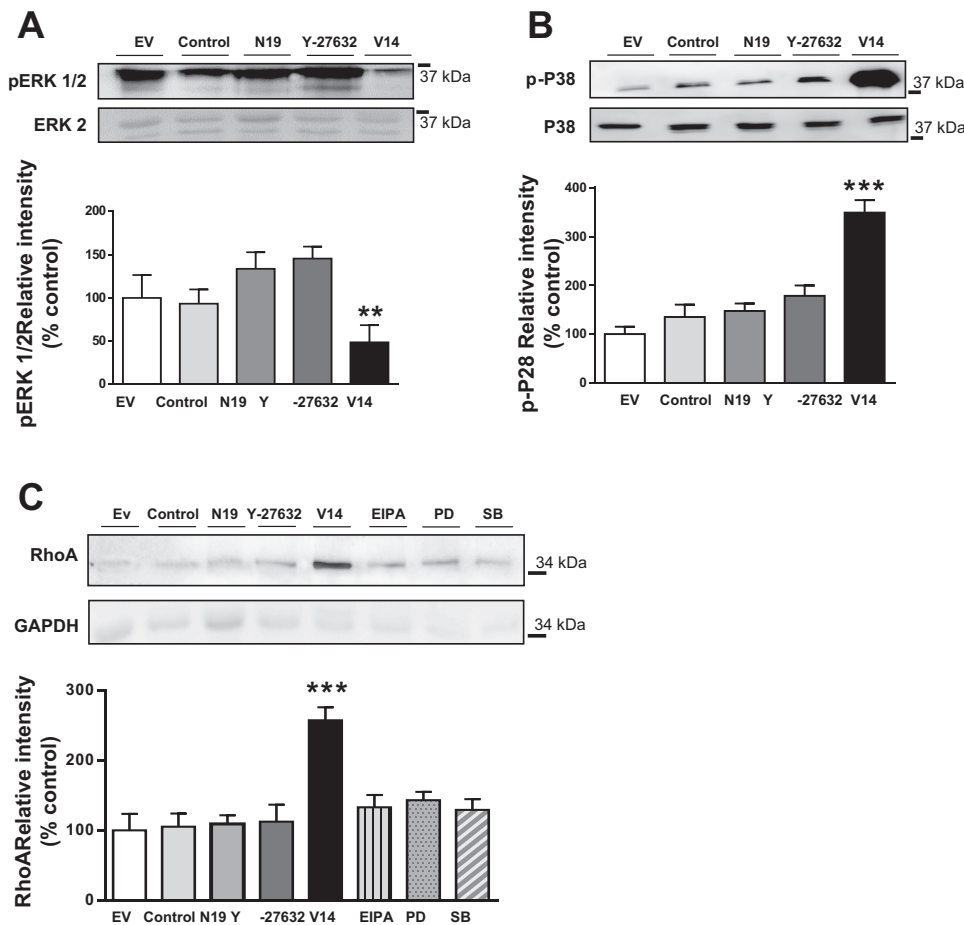
Fig. 6. Cross-talk between RhoA and the MAPK pathway. HK-2 cells were transfected with EGFP-RHOA wild type (WT) or mutants (constitutive active mutant EGFP-RHOA-V14 or constitutive inactive mutant EGFP-RHOA-N19). *A* and *B*: the active forms of ERK1/2 (*A*) and p38 (*B*) were determined using p-ERK- and p-p38-specific antibodies by Western blot analysis. Membranes were stripped and reprobed with total ERK1/2 and p38 antibodies. *C*: for RhoA analysis, HK-2 cells were transfected as previously described or preincubated with ROCK inhibitor (Y-27632; 10 mM), MEK1 inhibitor (PD; 30 mM), and p38 inhibitor (SB; 30 mM) for 60 min. The membrane fraction from the cell lysate was probed with RhoA antibody and GAPDH as a loading control. Expression levels on Western blots were determined using densitometric analysis. Data are expressed in the corresponding bar graph as means ± SE; $n = 3$. **$P < 0.01$. ***$P < 0.001$.

lumen, leading to axial cell deformation (12), an insult that triggers adaptive signals in response to stretch, resulting in tubular cell apoptosis and a lasting loss of functional renal parenchyma (3, 6). Most studies have demonstrated that apoptosis is accompanied by cytosol acidification (23), determining favorable conditions for apoptotic proteins, including caspase 3 activation. The control of pH_i is mostly regulated by NHE1. We (24) have previously reported renal tubule cell apoptosis after 14 days of UUO associated with NHE1 downregulation. Mechanical proximal tubule cell deformation can be reproduced by exposing HK-2 cells to cyclic mechanical stretch. We observed that NHE1 protein expression decreased gradually as time increased mechanical deformation, reaching the maximum decrease at 180 min of cyclic stretch, which is in accordance with the highest activation of caspase 3 and apoptosis induction. We further confirmed the direct participation of NHE1 in cell survival due to decreased Bcl-2 protein expression and higher caspase 3 after silencing the exchanger by NHE1 siRNA. Additionally, HK-2 cells with NHE1 pharmacological activity blockage showed higher apoptosis induction after mechanical stretch compared with nontargeted NHE1 cells. Moreover, after HK-2 NHE1 knockdown and subsequent mechanical deformation, later apoptosis induction exceeded the observed values in nontargeted NHE1 stretched cells and even compared with EIPA-treated stretched cells. These results shows that in EIPA-treated cells, early stretched cells could hit back the mechanical deformation probably due to the counter-

balancing activity of other pH_i regulators, but NHE1 downregulation showed increased time-dependent apoptosis with the highest values in later apoptosis, demonstrating that NHE1, through both activity and expression, participates in cell survival due to its function as a cell volume regulator and scaffold for signaling complexes. However, the specific mechanism of NHE1 inhibition in response to mechanical stretch has not been completely described. Cell survival and organization of the actin cytoskeleton are regulated through actin anchoring by NHE1 and supposedly by NHE1-dependent scaffolding of signaling proteins, despite NHE1 functioning as a pH_i regulator. However, little is known about the signal transduction pathway triggered by stretch and whether structural functions of NHE1 are important for mechanotransduction (22). Recent evidence demonstrates a direct regulation of NHE1 activity by the cytoskeleton and the reciprocity of NHE1 to regulate cytoskeletal dynamics (27). We focused on small GTPase RhoA because of its role in reorganization of the cortical cytoskeleton (17) and its relation with NHE1 as a scaffold protein (7, 8, 11). We demonstrated an early and progressive activation of RhoA in HK-2 cells exposed to cyclic stretch, showing that higher membrane-bound RhoA precedes NHE1 downregulation and reaches its maximal activation state at 180 min for mechanical deformation, in accordance with NHE1 downregulation and apoptosis induction. To confirm that RhoA signaling pathways are involved in NHE1 regulation, we inhibited RhoA using the ROCK inhibitor Y-27362 or a domi-
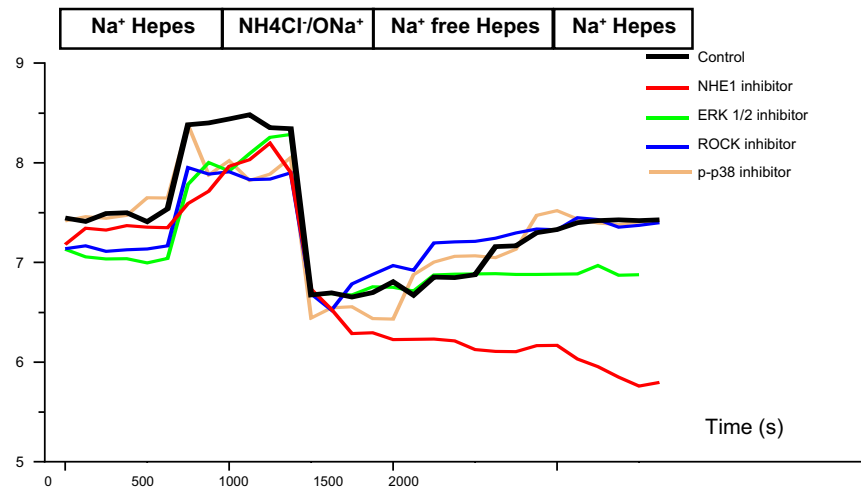
Fig. 7. Intracellular pH (pH$_i$) measurements in response to signaling pathway inhibitors. Na$^+$-dependent and Na$^+$-independent pH$_i$ measurements in HK-2 cells are shown. HK-2 cells were seeded in coverslips and incubated with NHE1 inhibitor (EIPA), ERK inhibitor (PD), ROCK inhibitor (Y-27632), and p38 inhibitor (SB) for 30 min and loaded with BCECF (10 μM). pH$_i$ recovery after cellular acidification with the NH$_4$Cl pulse technique was used to define NHE1 activity. pH$_i$ was measured microfluorometrically by exciting the dye alternately at 490 and 440 nm while monitoring the emission at 532 nm with a video-imaging system. Each experiment was calibrated for pH$_i$ using the nigericin/high-K$^+$ method, and the obtained ratios were converted to pH$_i$. Na$^+$-dependent pH$_i$ recovery rates in response to an acid load were calculated in HK-2 cells in the pH range of 6.80–7.00. Data are expressed as means ± SE; n is the number of cells investigated.

	Initial pH$_i$	Na$^+$-independent pH$_i$ recovery (pH/min)	Na$^+$-dependent pH$_i$ recovery (pH/min)	Final pH$_i$
Control	7.44±0.01	0.0202±0.002	0.0552± 0.003	7.42±0.02
NHE1 inhibitor (EIPA)	7.41±0.03	-0.0607±0.001	-0.0330±0.001	5.79±0.01
ERK 1/2 inhibitor (PD98059)	7.43±0.03	0.0204±0.002	-0.0006± 0.001	6.89±0.03
ROCK inhibitor	7.40±0.02	0.0528±0.003	0.0187±0.002	7.39±0.03
P-p38 inhibitor (SB203589)	7.41±0.02	0.0332±0.002	0.0517±0.001	7.42±0.02

nant negative RhoA mutant (EGFP-RHOA-N19). A constitutively active mutant was also probed (EGFP-RHOA-V14). We found that NHE1 protein expression was higher after RhoA inactivation, whereas EGFP-RHOA-V14 induced a reduction of NHE1 expression. NHE1 activity was similar to control HK-2 cells after 30 min of incubation with ROCK inhibitor, and absence of pH$_i$ acidification was observed after RhoA inhibition. These results confirm that RhoA activation is responsible for NHE1 downregulation, supporting the notion that it is an integral part of the signal transduction pathway involved in NHE1 regulation. Evidence in different cell types shows that stretch-induced activation of MAPK pathways involves either ERK1/2 or p38 MAPK (1, 32). In stretched HK-2 cells, we observed early ERK1/2 activation with an intensive phosphorylation decrease at 180 min of cyclic stretch. Conversely, p38 MAPK reached its maximal phosphorylation state at 180 min of mechanical deformation. Since the data found in the literature regarding the role of MAPK in NHE1 regulation differ according to cell type, we analyze the role of MAPK in stretch-induced apoptosis and NHE1 regulation in HK-2 cells. After p38 inhibition, an increase in NHE1 protein expression without caspase 3 activation was shown. On the other hand, ERK1/2 inhibition leads to decreased NHE1 expression and caspase 3 activation. Manipulation of MAPK activation also

affected NHE1 activity, showing diminished pH$_i$ recovery after ERK1/2 inhibition and NHE1 activity similar to control cells when HK2 cells were incubated with the p38 inhibitor. These results are in agreement with other authors showing that in renal tubule cells, p38 and ERK have been shown to be activated by stretch in vitro or in vivo after obstruction (25, 26) and that inhibition of ERK leads to NHE1 blockage (9). Altogether, our findings suggest that cyclic stretch activates different signaling pathways, possibly associating with each other, converging on an apoptotic response that includes NHE1 regulation. Searching for the underlying sequence that triggers tubular cell apoptosis in response to mechanical stretch that concludes with NHE1 downregulation, we attempted to elucidate how RhoA and MAPK pathways were related. When EGFP-RHOA-V14 was expressed in HK-2 cells, ERK1/2 activation was suppressed and p38 activity was increased, demonstrating that RhoA activation modifies the MAPK phosphorylation state. On the other hand, when HK-2 cells were incubated with either ERK1/2 inhibitor or p38 inhibitor, membrane-bound RhoA remained similar to nontreated HK-2 cells, demonstrating that RhoA is upstream of the MAPK signaling pathway. Taken together, our data obtained in human proximal tubule cells suggest that RhoA signaling pathway activation after mechanical stretch induces ERK1/2 inhibition and p38

activation, which downregulates NHE1 expression and activity and finally triggers caspase 3 activation and apoptosis induction.

DISCLOSURES

No conflicts of interest, financial or otherwise, are declared by the author(s).

AUTHOR CONTRIBUTIONS

Author contributions: V.B. and P.G.V. conception and design of research; V.B., A.F.G.L., V.C., M.E.B., and V.V.C. performed experiments; V.B., A.F.G.L., V.C., M.E.B., and V.V.C. analyzed data; V.B., A.F.G.L., V.V.C., and P.G.V. interpreted results of experiments; V.B. prepared figures; V.B. drafted manuscript; V.B. and P.G.V. edited and revised manuscript; V.B., A.F.G.L., V.C., M.E.B., and V.V.C. approved final version of manuscript.

REFERENCES

1. **Aikawa R, Nagai T, Kudoh S, Zou Y, Tanaka M, Tamura M, Akazawa H, Takano H, Nagai R, Komuro I.** Integrins play a critical role in mechanical stress-induced p38 MAPK activation. *Hypertension* 39: 233–238, 2002.
2. **Bianchini L, L'Allemain G, Pouyssegur J.** The p42/p44 mitogen-activated protein kinase cascade is determinant in mediating activation of the Na^+/H^+ exchanger (NHE1 isoform) in response to growth factors. *J Biol Chem* 272: 271–279, 1997.
3. **Bocanegra V, Rinaldi TM, Gil LA, Cacciamani V, Manucha W, Fornes M, Valles PG.** Angiotensin AT_1 receptor inhibition-induced apoptosis by RhoA GTPase activation and pERK1/2 signaling pathways in neonatal obstructive nephropathy. *Histol Histopathol* 27: 919–930, 2012.
4. **Bossy-Wetzel E, Green DR.** Detection of apoptosis by annexin V labeling. *Methods Enzymol* 322: 15–18, 2000.
5. **Bradford MM.** A rapid and sensitive method for the quantitation of microgram quantities of protein utilizing the principle of protein-dye binding. *Anal Biochem* 72: 248–254, 1976.
6. **Cachat F, Lange-Sperandio B, Chang AY, Kiley SC, Thornhill BA, Forbes MS, Chevalier RL.** Ureteral obstruction in neonatal mice elicits segment-specific tubular cell responses leading to nephron loss. *Kidney Int* 63: 564–575, 2003.
7. **Cardone RA, Bagorda A, Bellizzi A, Busco G, Guerra L, Paradiso A, Casavola V, Zaccolo M, Reshkin SJ.** Protein kinase A gating of a pseudopodial-located RhoA/ROCK/p38/NHE1 signal module regulates invasion in breast cancer cell lines. *Mol Biol Cell* 16: 3117–3127, 2005.
8. **Cardone RA, Busco G, Greco MR, Bellizzi A, Accardi R, Cafarelli A, Monterisi S, Carratu P, Casavola V, Paradiso A, Tommasino M, Reshkin SJ.** HPV16 E7-dependent transformation activates NHE1 through a PKA-RhoA-induced inhibition of p38alpha. *PLOS ONE* 3: e3529, 2008.
9. **Carraro-Lacroix LR, Ramirez MA, Zorn TM, Reboucas NA, Malnic G.** Increased NHE1 expression is associated with serum deprivation-induced differentiation in immortalized rat proximal tubule cells. *Am J Physiol Renal Physiol* 291: F129–F139, 2006.
10. **Denker SP, Huang DC, Orlowski J, Furthmayr H, Barber DL.** Direct binding of the Na-H exchanger NHE1 to ERM proteins regulates the cortical cytoskeleton and cell shape independently of H^+ translocation. *Mol Cell* 6: 1425–1436, 2000.
11. **Di Ciano-Oliveira C, Sirokmany G, Szaszi K, Arthur WT, Masszi A, Peterson M, Rotstein OD, Kapus A.** Hyperosmotic stress activates Rho: differential involvement in Rho kinase-dependent MLC phosphorylation and NKCC activation. *Am J Physiol Cell Physiol* 285: C555–C566, 2003.
12. **Gaudio KM, Siegel NJ, Hayslett JP, Kashgarian M.** Renal perfusion and intratubular pressure during ureteral occlusion in the rat. *Am J Physiol Renal Fluid Electrolyte Physiol* 238: F205–F209, 1980.
13. **Geibel J, Giebisch G, Boron WF.** Angiotensin II stimulates both Na^+-H^+ exchange and Na^+. *Proc Natl Acad Sci USA* 87: 7917–7920, 1990.
14. **Gil Lorenzo AF, Bocanegra V, Benardon ME, Cacciamani V, Valles PG.** Hsp70 regulation on Nox4/p22^{phox} and cytoskeletal integrity as an effect of losartan in vascular smooth muscle cells. *Cell Stress Chaperones* 19: 115–134, 2014.
15. **Gobe GC, Axelsen RA.** Genesis of renal tubular atrophy in experimental hydronephrosis in the rat. Role of apoptosis. *Lab Invest* 56: 273–281, 1987.
16. **Kaplan MR, Plotkin MD, Brown D, Hebert SC, Delpire E.** Expression of the mouse Na-K-2Cl cotransporter, mBSC2, in the terminal inner medullary collecting duct, the glomerular and extraglomerular mesangium, and the glomerular afferent arteriole. *J Clin Invest* 98: 723–730, 1996.
17. **Kapus A, Di CC, Sun J, Zhan X, Kim L, Wong TW, Rotstein OD.** Cell volume-dependent phosphorylation of proteins of the cortical cytoskeleton and cell-cell contact sites. The role of Fyn and FER kinases. *J Biol Chem* 275: 32289–32298, 2000.
18. **Kapus A, Grinstein S, Wasan S, Kandasamy R, Orlowski J.** Functional characterization of three isoforms of the Na^+/H^+ exchanger stably expressed in Chinese hamster ovary cells. ATP dependence, osmotic sensitivity, and role in cell proliferation. *J Biol Chem* 269: 23544–23552, 1994.
19. **Khaled AR, Moor AN, Li A, Kim K, Ferris DK, Muegge K, Fisher RJ, Fliegel L, Durum SK.** Trophic factor withdrawal: p38 mitogen-activated protein kinase activates NHE1, which induces intracellular alkalinization. *Mol Cell Biol* 21: 7545–7557, 2001.
20. **Khan S, Cleveland RP, Koch CJ, Schelling JR.** Hypoxia induces renal tubular epithelial cell apoptosis in chronic renal disease. *Lab Invest* 79: 1089–1099, 1999.
21. **Khan S, Koepke A, Jarad G, Schlessman K, Cleveland RP, Wang B, Konieczkowski M, Schelling JR.** Apoptosis and JNK activation are differentially regulated by Fas expression level in renal tubular epithelial cells. *Kidney Int* 60: 65–76, 2001.
22. **Kung C.** A possible unifying principle for mechanosensation. *Nature* 436: 647–654, 2005.
23. **Lagadic-Gossmann D, Huc L, Lecureur V.** Alterations of intracellular pH homeostasis in apoptosis: origins and roles. *Cell Death Differ* 11: 953–961, 2004.
24. **Manucha W, Carrizo L, Ruete C, Valles PG.** Apoptosis induction is associated with decreased NHE1 expression in neonatal unilateral ureteric obstruction. *BJU Int* 100: 191–198, 2007.
25. **Masaki T, Foti R, Hill PA, Ikezumi Y, Atkins RC, Nikolic-Paterson DJ.** Activation of the ERK pathway precedes tubular proliferation in the obstructed rat kidney. *Kidney Int* 63: 1256–1264, 2003.
26. **Nguyen HT, Hsieh MH, Gaborro A, Tinloy B, Phillips C, Adam RM.** JNK/SAPK and p38 SAPK-2 mediate mechanical stretch-induced apoptosis via caspase-3 and -9 in NRK-52E renal epithelial cells. *Nephron Exp Nephrol* 102: e49-e61, 2006.
27. **Putney LK, Denker SP, Barber DL.** The changing face of the Na^+/H^+ exchanger, NHE1: structure, regulation, and cellular actions. *Annu Rev Pharmacol Toxicol* 42: 527–552, 2002.
28. **Riveline D, Zamir E, Balaban NQ, Schwarz US, Ishizaki T, Narumiya S, Kam Z, Geiger B, Bershadsky AD.** Focal contacts as mechanosensors: externally applied local mechanical force induces growth of focal contacts by an mDia1-dependent and ROCK-independent mechanism. *J Cell Biol* 153: 1175–1186, 2001.
29. **Ryan MJ, Johnson G, Kirk J, Fuerstenberg SM, Zager RA, Torok-Storb B.** HK-2: an immortalized proximal tubule epithelial cell line from normal adult human kidney. *Kidney Int* 45: 48–57, 1994.
30. **Sumpio BE, Banes AJ.** Response of porcine aortic smooth muscle cells to cyclic tensional deformation in culture. *J Surg Res* 44: 696–701, 1988.
31. **Wagner CA, Lukewille U, Valles P, Breton S, Brown D, Giebisch GH, Geibel JP.** A rapid enzymatic method for the isolation of defined kidney tubule fragments from mouse. *Pflügers Arch* 446: 623–632, 2003.
32. **Wang JG, Miyazu M, Matsushita E, Sokabe M, Naruse K.** Uniaxial cyclic stretch induces focal adhesion kinase (FAK) tyrosine phosphorylation followed by mitogen-activated protein kinase (MAPK) activation. *Biochem Biophys Res Commun* 288: 356–361, 2001.